THE JOURNAL OF PHYSICAL CHEMISTRY A

© Copyright 2002 by the American Chemical Society VOLUME 106, NUMBER 3, JANUARY 24, 2002

LETTERS

Isomerization and Melting-Like Transition of Size-Selected Water Nonamers

Jesko Brudermann and Udo Buck*

Max-Planck-Institut für Strömungsforschung, Bunsenstrasse 10, D-37073 Göttingen, Germany

Victoria Buch

The Fritz Haber Institute for Molecular Dynamics, The Hebrew University, Jerusalem 91904, Israel

Received: August 2, 2001; In Final Form: October 23, 2001

The vibrational OH-stretch spectra of size-selected pure water $(H_2O)_9$ clusters, measured at two different temperatures, have been used to identify isomeric transitions. The broad, featureless high-temperature, liquid-like spectrum resembles that of water, while the structured low-temperature, solid-like spectrum differs appreciably from that of ice. Accompanying calculations suggest that the low-temperature spectra originate from two cube-like structures. The high-temperature spectra appear to be above an isomeric transition to more open amorphous arrangements of fused three- to five-membered rings.

Introduction

The concept of phase transitions in small clusters is essentially based on many computer simulations that have been carried out for a number of selected species ranging from van der Waals and hydrogen bonded systems to ionic bonds and metals.[1−3] The solid-like to liquid-like transitions are usually described as isomerization between a multitude of isomers. Experimental evidence for these processes is still quite rare, since size selection and temperature are prerequisites that are difficult to fulfill. The most detailed experiments up to now have been carried out for metal cluster ions that have been studied over a large range of sizes and temperatures.[4] For neutral molecular systems, the very special arrangement of rare gases and aromatic molecules have been investigated.[5] For hydrogen-bonded systems, an isomeric transition of methanol hexamers was reported by us several years ago.[6] Here the different signatures of the infrared spectrum were used for identification of the isomers. Results for distributions of large water clusters were also reported using electron diffraction.[7,8]

In this letter we would like to report another example of such a transition for water nonamers $(H_2O)_9$. Recently, we sucessfully measured the OH-stretch spectra of $(H_2O)_n$ clusters in the size range from $n = 7$ to $n = 10$.[9,10] The clusters were size selected using the atomic beam deflection method[11] and the spectra were obtained by the depletion of the signal caused by the predissociation of the cluster upon the IR excitation.[12] In a very detailed effort, the experimental spectra were explained by combined high-level ab initio calculations and simulations based on a polarizable model potential.[13] The central building blocks in this size range are the octamer cubes, which consist of four alternating 3-coordinated double donor−single acceptor (DDA) and four single donor−double acceptor (DAA) water molecules. They give rise to a DDA band near 3550 cm^{-1}, and a bonded OH band of DAA molecules near 3100 cm^{-1}. Together with the band of the free OH near 3720 cm^{-1} this results in three well-separated bands that also persist for the $n = 9$ and $n = 10$ clusters (see Figure 1, top). In contrast, the heptamer exhibits a series of lines originating from individual bonds. For closely related studies of OH spectroscopy of water clusters in this size range, connected to benzene or phenol, see refs 14−16.

To provide the access to other than the lowest energy isomers, we have to increase the cluster temperature. This is achieved

10.1021/jp012986k CCC: $22.00 © 2002 American Chemical Society
Published on Web 12/27/2001

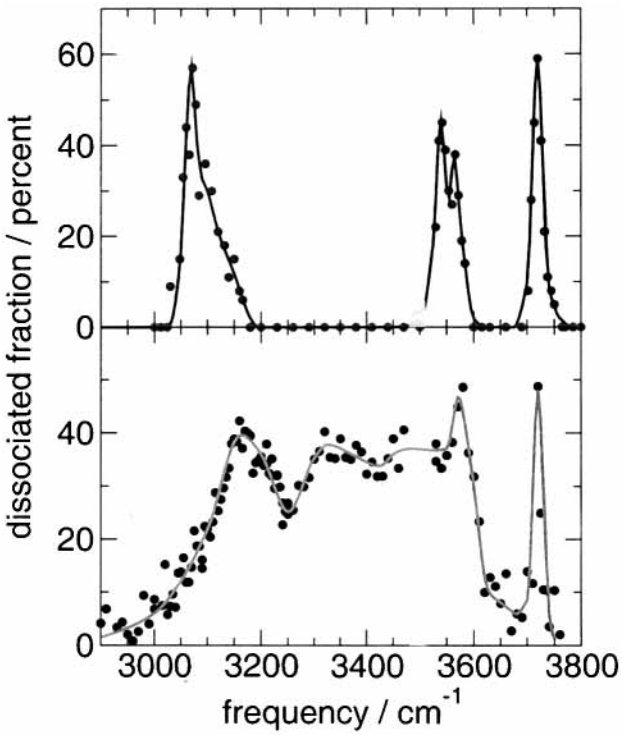

Figure 1. Top: Measured low-temperature OH-stretch spectrum of $(H_2O)_9$ from ref 9. Bottom: Measured high-temperature OH-stretch spectrum of $(H_2O)_9$. The experimental conditions for both experiments are given in Table 1. The solid lines are guides to the eye.

in the present experiment by changing the source conditions of the cluster beam in an appropriate manner. The cluster temperature is estimated from a simple relaxation model and is found to be 186 K, in contrast to the value 69 K that was determined for the previously published experiment.[9] The resulting spectrum is quite broad without any indication of a single resolved band aside from that of the free OH-stretch (see Figure 1, bottom). By accompanying calculations employing classical simulations of cluster dynamics and quantum evaluations of spectra for selected minima, the broadening is proposed to be due to an isomeric transition to more open amorphous structures of higher energy. By comparison with experimental results, a similar increase of the cluster temperature is obtained. The implications of a solid-like to a liquid-like transition will be discussed, and these results will also be compared with the spectra of ice and water.

Experimental Section

The experimental method we apply is a combination of size selection by momentum transfer in a scattering experiment with atoms, with the infrared depletion technique.[11,12] In the first step the different clusters are dispersed into different angles according to their masses and detected by a mass spectrometer. This technique has been developed in our laboratory in Göttingen and applied to cluster sizes up to $n = 13$.[17] Then the OH-stretch vibrational mode of the water molecules is excited by infrared laser radiation. The detector records the depletion in the cluster signal caused by the clusters which are dissociated by the absorbed radiation.

The experimental setup consists of a crossed molecular beams apparatus with an angular dependent detection of the scattered beam of a resolution of 0.2° using electron impact ionization and mass selection in a quadrupole mass filter.[18] The water

TABLE 1: Characteristic Data for the Two $(H_2O)_9$ Cluster Beams

property	this work	ref 10
nozzle diameter (μm)	146	313[a]
temperature T_0 (K)	343	355
pressure (bar)	1.0	2.3
mixture in He (%)	20.0	16.7
velocity (m/s)	1466	1654
cluster temperature (K)	69	186

[a] Equivalent diameter of a conical nozzle.

clusters are generated by an adiabatic expansion of a dilute mixture of 20% water vapor at 343 K with helium as carrier gas at 1.0 bar through a nozzle with 146 μm diameter. For the size selection, the water cluster beam is deflected by a helium beam.[11] The helium beam is produced by the expansion of the gas under the pressure of 30 bar through a nozzle of 30 μm diameter at room temperature. The detector is set on the largest possible scattering angles for $n = 9$, $\Theta_9 = 4.0°$ in our experimental arrangement. This expells all larger clusters. Smaller clusters are excluded by means of the mass spectrometer operated at the masses of the corresponding protonated $(H_2O)_8H^+$ ions of mass $m = 145$ u. The achieved energy and angular resolution is high enough to separate the $n = 9$ contribution from the next larger ones. In this way complete size selection is achieved. For the excitation of the OH-stretch mode, a home-built optical parametric oscillator was used as coherent light source.[19] The tuning range is between 2400 and 3800 cm^{-1} at an average output energy of 2 mJ/pulse, a resolution of 0.2 cm^{-1}, and a repetition rate of 20 Hz. Because of water impurities in the crystal, our arrangement has an intensity gap between 3460 and 3500 cm^{-1}.

Cluster Temperature

The only experimental information we have about the cluster temperature is that of the source conditions and the final beam parameters of the cluster. They are presented in Table 1 together with those observed for the spectrum already published for cold $(H_2O)_9$.[9] To get a reliable estimation of the cluster temperature, we take advantage of the fact that our expansions are dilute mixtures in helium so that the cluster formation can be separated from the collisional relaxation of the clusters that determines the temperature. Thus we first simulated the cluster formation in the adiabatic expansion in the spirit of the published work[20,21] using the recently published values of the rates for water cluster formation and decay.[22] The cluster generation of $n = 9$ is completed at about $x = 4$ reduced nozzle diameters. In a second step, we calculated the reduced cluster temperature $T_{red} = T_c/T'_0$ from the relaxation of the excited clusters $dT_{red}/dt = kn(T - T_{red})$ by collisions with helium atoms, where T'_0 is the initial local temperature at the point of the cluster formation. Here the collision rate, k, with He and the helium density, n, enter. This method is similar to the concept of the relaxation of the internal degrees of freedom by collisions with the carrier gas during the expansion, as was described by Miller.[23] The results for the two experiments are $T_c/T'_0 = 0.78$ for the warm clusters of this experiment and $T_c/T'_0 = 0.29$ for the previous experiment. While the amount of cluster formation in the two expansions is quite similar in the two cases, the pressure differs by a factor of 2.3. This leads to a much less effective cooling of the water clusters in the former case and a higher reduced temperature results.

The final step is the calculation of the local temperature T'_0. There is a small contribution from the local temperature of the

isentropic expansion of about 19 K, but the main part should come from the fraction of the energy released in the condensation process. To get a reliable estimation of this energy, we make use of a further result of our experiments that is the difference in the final velocity of the cluster beams. According to the typical energy balance of the expansion with the source temperature T_0 and the final final temperature T

$$\langle C_p \rangle T_0 = \langle C_p \rangle T + \Sigma x_c C_c T_c + 0.5 \langle m \rangle u^2 - E_{con} \qquad (1)$$

where $\langle C_p \rangle = \Sigma x_i C_p$ is the average specific heat at constant pressure for the different fractions x_i in the beam, u is the velocity averaged over the different beam particles, and E_{con} is the condensation energy. We expect that clusters with a higher temperature T_c should exhibit smaller velocities for otherwise constant conditions. This is indeed observed, since the water nonamers produced in this work are 190 m/s slower than those generated in ref 9. From this measured velocity difference we calculate a temperature $T'_0 = 239$ K by keeping the other three terms constant. From this result we get for the cluster temperatures $T_c = 69$ and 186 K, respectively.

Calculations

The calculations included (a) classical trajectory simulations of cluster structure and dynamics as a function of the (classical) temperature, (b) computation of minimum energy structures, with points along the trajectory as starting points, (c) quantum calculations of temperature-dependent spectra of selected minima, employing a model that was devised in the past for the analysis of $n = 7-10$ clusters.[13] The calculation employed a modification[24] of the empirical polarizable water potential proposed in ref 25 (henceforth EMP). The EMP potential was shown to provide a reasonable description of the different water phases (solid, liquid, and clusters). In the minimizations and the classical trajectory simulations the molecules were treated as rigid bodies. The trajectories employed the SHAKE/Verlet algorithm[26] and a time step of 40 atomic units; the two lowest cage minima[13,15] (Figure 2, upper panel) were used as a starting point. These structures were heated by molecular dynamics to a desired temperature, and a trajectory of the length of 1−4 ns was run. Structures were minimized at intervals of 5 ps.

It was found that some minimum energy structures appeared in simulations more often than others. For these structures, the spectra were evaluated quantum-mechanically using a model described in ref 13. (Molecular dynamics calculations of spectra are problematic due to artifacts of the classical treatment; see, e.g. ref 27.) To translate minimum energy structures to the spectra, the stretch Hamiltonian was diagonalized in the Morse exciton basis. The OH bonds were treated as a collection of inter- and intramolecularly coupled local oscillators. The bond frequency ω was assumed to be determined by the electric field component $E_{||}$ at the H-atom along the OH bond, as suggested by ab initio studies of ref 28. The function $\omega(E_{||})$ was constructed by fitting to experimental data, mostly to the $n = 7-8$ spectra.[13] The relation between OH-stretch and intermolecular motion was assumed self-consistent-field-like. That is, the bond stretch constant k_{bond} was averaged over the intermolecular motion represented by the normal modes. For the purpose of averaging, the intermolecular vibrational wave function was approximated as a product of harmonic oscillator eigenfunctions. The averaging was carried out numerically, using fourteen point Gauss-Hermite integration. The occupation numbers of the different intermolecular modes were selected at random from the thermal distribution. This (limited) use of the harmonic approximation in the calculations of the effect of temperature on the OH-stretch spectra is, of course, approximate. However, the resulting very significant thermal broadening of the spectra is likely to be correct.

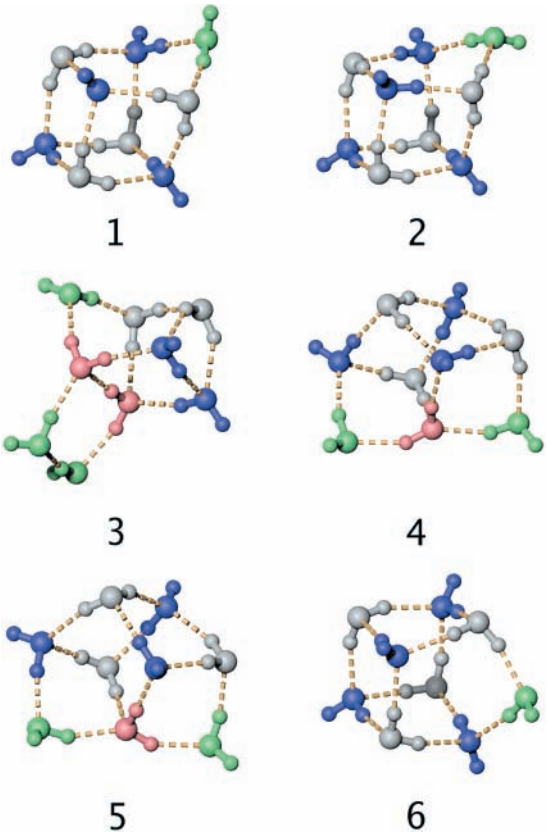

Figure 2. Structures of $(H_2O)_9$ minima listed in Table 2. Upper part: the two lowest energy structures (**1**, **2**). Lower part: four examples of the family of high-energy structures (**3**−**6**). Color code of the coordination number: DA, green; DDA, gray; DAA, blue; DDAA, red.

Results and Discussion

The measured spectrum at the higher temperature is shown in the lower part of Figure 1. For comparison, the result obtained previously for the $(H_2O)_9$ at the lower temperature is presented in the upper part of Figure 1. Aside from the narrow peak of the free OH-stretch at 3720 cm^{-1}, there is no agreement within the rest of the spectra. In the case of the spectrum at higher temperature the whole range from 3200 to 3500 cm^{-1} is covered with intensity, which is missing in the other spectrum. While the DDA band at 3550 cm^{-1} starts at the same position as does the spectrum at lower temperature, there is a remarkable shift to larger values of the DAA band from 3060 to about 3150 cm^{-1} in the high-temperature spectrum.

The two lowest energy structures of the nonamer, obtained with the EMP potential, are shown at the top of Figure 2. Their minimum energies are presented together with other characteristic features in Table 2. They can be viewed as fused pentamer and tetramer, with the OH bonds within the two rings oriented either in the opposite or the same direction (N_{opp} and N_{same} isomers). The two structures were investigated by us in detail in the past[13] (including diffusion Monte Carlo (DMC) and ab initio calculations). Each structure is a double well, corresponding to two different orientations of the dangling-H in the DA molecule (the orientations differ by about 100°). The barrier is low; in simulations at 60 K both minima of the double well were probed. The connectivity network was maintained through-

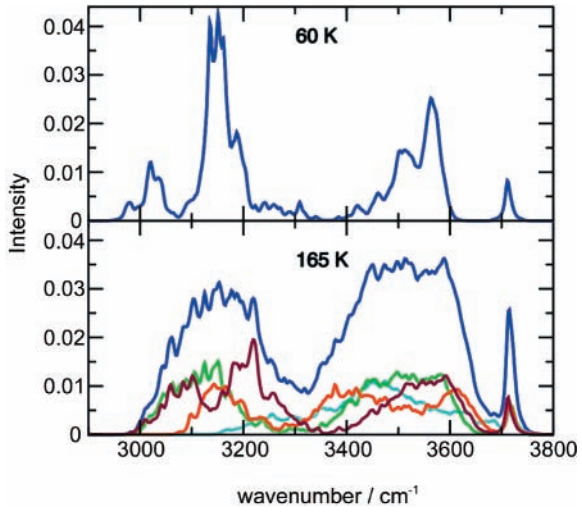

Figure 3. Calculated OH spectra for different temperatures. Upper panel: calculation at 60 K that mainly reflects contributions of the two low-lying isomers **1** and **2**. Lower panel: calculation at 165 K. The solid blue line is the sum of the contributions from the isomers **3** (teal), **4** (dark green), **5** (red), and **6** (brown) shown in Figure 2.

TABLE 2: Properties of Different Minima of $(H_2O)_9$, Obtained with the EMP Potential

no.	energy E (kcal/mol)	dipole moment (debye)	rotational constants (MHz) A	B	C
1	−80.54	1.65	786	630	566
2	−80.24	1.86	773	641	571
3	−75.31	3.93	826	515	473
4	−77.89	2.63	849	612	507
5	−78.37	2.84	838	618	499
6	−79.74	1.80	768	640	567

out the simulation; i.e., interchange of molecules within the structures did not occur. Since simulations remained localized in the vicinity of the respective two isomers, it makes sense to treat them as separate species. The relative contribution of N_{opp} and N_{same} at 60 K was estimated as 2.4:1. The corresponding calculated spectrum, shown in the upper part of Figure 3, displays broadended, but still separate, features for DAA, DDA, and dangling OH, in accord with experiment.[29] In contrast to the conclusion in refs 9 and 13, apparently both low-lying isomers contribute to the spectrum.

Another way to view the low-energy isomers is as products of insertion of a DA molecule to either D_{2d} or S_4 octamer cubes. The different possible products of such insertion were discussed in detail in the DFT study of ref 15. That study reported resonant ion-dip infrared spectra of low-temperature nonamer complexes with benzene; the nonamer structure in the observed isomers was also assigned to N_{opp} and N_{same} isomers.

As the simulation temperature was raised to 140 K, the trajectories were still localized predominantly near N_{opp} and N_{same} structures; however, neighboring higher energy versions of the cube were accessed as well. Near 165 K a qualitative change occurred: the cluster left the vicinity of the initial low-energy structure. In the course of each of four calculated 1.5−2.0 ns trajectories, the cluster became localized in the vicinity of one dominant high-energy structure, while visiting neighboring minima as well. The four structures are shown in the lower part of Figure 2. One is a high-energy version of the cube, the remaining three correspond to more open "amorphous" structures including 2- to 4-coordinated water molecules, and three- to five-membered rings. The qualitative effect of the structure distribution is assessed by overlapping the four corresponding

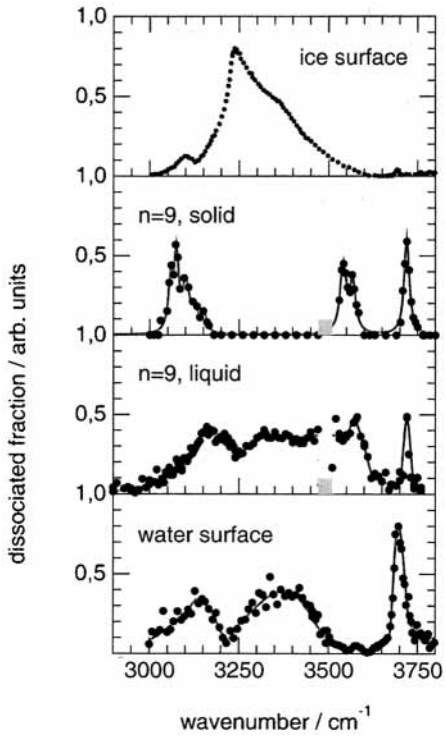

Figure 4. Comparison of the measured OH-stretch spectra of $(H_2O)_9$ and the measured surface spectra of water and ice. From the top to the bottom: surface spectrum of ice from ref 38; measured low-temperature OH-stretch spectrum of $(H_2O)_9$ from ref 9; measured high-temperature OH-stretch spectrum of $(H_2O)_9$; surface spectrum of water from ref 37.

spectra. The result is shown in the lower part of Figure 3. It is seen that each spectrum is thermally broadened (since at 165 K a large number of vibrational intermolecular states is populated). The sum of the four spectra is not unlike the measured high-T spectrum, except that the calculated dip in the spectrum is too large.

Further theoretical investigation is needed, including a fully quantum-mechanical treatment of structure and dynamics of this hydrogen-rich cluster, a full description of the structure distribution accessed at high T, and the dependence on the potential function. Still, the present results suggest that, despite the thermal broadening, a single structure is insufficient to reproduce the observed broad flat-topped high-temperature spectrum. Thus a transition to a distribution of high-energy structures is indicated. The calculated transition temperature is somewhat lower than the value derived from experiment; however, this discrepancy could easily originate from inaccuracies of the potential and of the use of classical dynamics as well as from the evaluation of the cluster temperature.

This type of transition has been calculated for water clusters in this size range by several groups.[30−36] They all predict a sharp melting transition for $(H_2O)_8$, but the temperature depends sensitively on the model potential employed with an averaged value centered around 200 K.[34] For $(H_2O)_9$ only one calculation is available, which gives 105 K, a value that is probably too low due to the simple potential model used.[30] The necessary condition for a sharp solid-like to liquid-like transition to occur is a large energy gap between the global minimum (or a group of low-lying minima) and the higher lying minima. Pedulla and Jordan[34] observed for the water octamer differences larger than 1.8 kcal/mol. The energy gap between the cubic low-energy structures and the amorphous high-energy isomers accessed in the present study by the nonamers, is aside for isomer 6, in this

range. This is confirmed by the observation made in a very recent investigation of the dynamical aspects of these transitions for water octamers.[36] They found that in the melting transition their chosen order parameter, the ratio between the smallest and the biggest moment of inertia, varies from 1.25 for the solid-like to 1.8 for the liquid-like behavior. The correponding values for the two groups of isomers in the present study are 1.35 and 1.74, respectively, again with the exception of isomer 6. Thus we conclude that very probably the measured high-temperature spectrum reflects a melting transition.

For comparison, we have also plotted recent measurements of the spectrum of the surface of water in the liquid state obtained by sum frequency generation (SFG)[37] and of the surface of nanocrystalline ice.[38] The comparison with surface spectra is certainly more realistic than that with bulk spectra, since these small clusters are all on the surface. The similarities that are observed in the liquid case are quite remarkable, although the comparison should be carried out with some caution, since the intensity of surface modes observed by SFG is determined by different transiton matrix elements. In contrast, the infrared spectra of ice nanocrystal surfaces and the solid-like nonamer look completely different, which is not surprising considering that the main contribution in the former case is from 4-coordinated inner surface molecules instead of from 3-coordinated molecules of a cube-like structure.

In summary, the new measurement of the OH-stretch spectrum of $(H_2O)_9$ at higer temperature exhibits the ingredients of a solid-like to liquid-like transition. The simulations indicate that the spectral broadening and the flat top behavior are due to a superposition of thermally broadened spectra of a number of high-energy isomers. In contrast to the two low-energy structures derived from the compact octamer cubes, the high-energy structures are more open and include fused three- to five-menbered rings. The estimated temperature of the cluster in the liquid-like spetra and thus the upper limit for the melting transition is in the range between 165 K (simulation) and 186 K (experiment). It is lower than that calculated for the more symmetric octamers and much lower than that of the bulk.

Acknowledgment. We thank the Deutsche Forschungsgemeinschaft and the Israel Science Foundation for financial support.

References and Notes

(1) Berry, R. S.; Beck, T. L.; Davies, H. L.; Jellinek, J. *Adv. Chem. Phys.* **1988**, *70*, 74.

(2) Berry, R. S. In *The Chemical Physics of Atomic and Molecular Clusters*; Scoles, G., Ed.; North-Holland: Amsterdam, 1990; p 23.

(3) Jortner, J.; Scharf; D.; Ben-Horin, N.; Even, U.; Landman, U. In *The Chemical Physics of Atomic and Molecular Clusters*; Scoles, G., Ed.; North-Holland: Amsterdam, 1990; p 43.

(4) Schmidt, M.; Kusche, R.; Hippler, T.; Donges, J.; Kronmüller, W.; von Issendorf, B.; Haberland, H. *Phys. Rev. Lett.* **2001**, *86*, 1191. Kusche, R.; Hippler, T.; Schmidt, M.; von Issendorf, B.; Haberland, H. *Nature (London)* **1998**, *393*, 212.

(5) Leutwyler, S.; Bösinger, J. *Chem. Rev.* **1990**, *90*, 489.

(6) Buck, U.; Ettischer, I. *J. Chem. Phys.* **1994**, *100*, 6974.

(7) Torchet, G.; Schwartz, P.; Farges, J.; de Feraudy, M. F.; Raoult, B. *J. Chem. Phys.* **1983**, *79*, 6196.

(8) Huang, J.; Bartell, L. S. *J. Phys. Chem.* **1995**, *99*, 3924.

(9) Buck, U.; Ettischer, I.; Melzer, M.; Buch, V.; Sadlej, J. *Phys. Rev. Lett.* **1998**, *80*, 2578.

(10) Brudermann, J.; Melzer, M.; Buck, U.; Kazimirski, J.; Sadlej, J.; Buch, V. *J. Chem. Phys.* **1999,** *110*, 10649.

(11) Buck U.; Meyer, H. *J. Chem. Phys.* **1986**, *84*, 4854.

(12) Buck, U. *J. Phys. Chem.* **1994**, *98*, 5190.

(13) Sadlej, J.; Buch, V.; Kazimirski, J.; Buck, U. *J. Phys. Chem. A* **1999,** *103*, 4933.

(14) (a) Pribble, R. N.; Zwier, T. S. *Science* **1994**, *265*, 75. (b) Gruenloh, C. J.; Carney, J. R.; Arrington, C. A.; Zwier, T. S.; Fredericks, S. Y.; Jordan, K. D. *Science* **1997**, *276*, 1678.

(15) Gruenloh, C. J.; Carney, J. R.; Hagemeister, F. C.; Zwier, T. S.; Wood, J. T., III; Jordan, K. D. *J. Chem. Phys.* **2000**, *113*, 2290.

(16) Janzen, C.; Spangenberg, D.; Roth, W.; Kleinermanns, K. *J. Chem. Phys.* **1999**, *110*, 9898.

(17) Buck U.; Ettischer, I. *Faraday Discuss. Chem. Soc.* **1994**, *97*, 215.

(18) Buck, U.; Gu, X. J.; Lauenstein, C.; Rudolph, A. *J. Chem. Phys.* **1990**, *92*, 6017.

(19) Buck, U.; Ettischer, I. *J. Chem. Phys.* **1998**, *108*, 33.

(20) Wolf, K.; Kuge, K. H.; Kleinermanns, K. *Z. Phys. D* **1991**, *18*, 409.

(21) Bartell, L. S. *J. Phys. Chem. A* **1990**, *94*, 5102.

(22) Kathmann, S.; Schenter, G. K.; Garret, B. C. *J. Chem. Phys.* **1998**, *108*, 33.

(23) Miller, D. R. In *Atomic and Molecular Beam Methods*; Scoles, G., Ed.; North-Holland: Amsterdam, 1990; p 14.

(24) Buch, V.; Sandler, P.; Sadlej, J. *J. Phys. Chem. B* **1998**, *102*, 8641.

(25) Kuwajima, S.; Warshel, A. *J. Phys. Chem.* **1990**, *94*, 460.

(26) McCammon, J. A. Harvey, S. C. *Dynamics of Proteins and Nucleic Acids*; Cambridge University Press: Cambridge, U.K., 1987.

(27) Johnson, W. G.; Buch, V.; Trenary, M. *J. Chem. Phys.* **1990**, *93*, 9167.

(28) Hermansson, K.; Lingren, J.; Probst, M. M. *Chem. Phys. Lett.* **1995**, *233*, 371.

(29) We note that the agreement refers to the shape of the spectra and not to the absolute scale that is shifted compared to the published calculations in ref 14 for $T = 0$ K due to a calibration error.

(30) Farantos, S. C.; Kapetanikis, S.; Vegiri, A. *J. Phys. Chem.* **1993,** *97*, 12158.

(31) Vegiri A.; Farantos, S. *J. Chem. Phys.* **1993**, *98*, 4066.

(32) Wales, D. J.; Ohmine, I. *J. Phys. Chem.* **1993**, *98*, 7245.

(33) Tsai, C. J.; Jordan, K. D. *J. Chem. Phys.* **1993**, *99*, 6957.

(34) Pedulla, J. M.; Jordan, K. *Chem. Phys.* **1998**, *239*, 593.

(35) Rodriguez, J.; Laria, D.; Marceca, E.; Estrin, D. A. *J. Chem. Phys.* **1999**, *110*, 9039.

(36) Laria, D.; Rodriguez, J.; Dellago, C.; Chandler, D. *J. Phys. Chem. A* **2001**, *105*, 2646.

(37) Baldelli, S.; Schnitzer, C.; Campbell, D. J.; Shultz, M. J. *J. Phys. Chem. B* **1999**, *103*, 2789.

(38) Devlin, J. P.; Sadlej, J.; Buch, V. *J. Phys. Chem. A* **2001**, *105*, 974.